

1 Tracing glacial disintegration from the LIA to the present using a LIDAR-based hi-res glacier inventory
2 in Austria

3

4

5

6

7 Andrea Fischer¹, Bernd Seiser¹, Martin Stocker Waldhuber^{1,2}, Christian Mitterer¹, Jakob
8 Abermann^{3,4}

9 Correspondence to: Andrea Fischer (andrea.fischer@oeaw.ac.at)

10

11 [1] {Institute for Interdisciplinary Mountain Research, Austrian Academy of Sciences,
12 Technikerstrasse 21a, 6020 Innsbruck, Austria}

13 [2] {Institut für Geowissenschaften und Geographie, Physische Geographie, Martin-Luther-
14 Universität Halle-Wittenberg, Von-Seckendorff-Platz 4, 06120 Halle, Germany}

15 [3] {Commission for Geophysical Research, Austrian Academy of Sciences}

16 [4] {now at Asiaq - Greenland Survey, 3900 Nuuk, Greenland}

17

18

19

20

21

22

23

24

25 **Abstract**

26

27 Glacier inventories provide the basis for further studies on mass balance and volume change,
28 relevant for local hydrological issues as well as for global calculation of sea level rise. In this
29 study, a new Austrian glacier inventory has been compiled, updating data from 1969 (GI 1)
30 and 1998 (GI 2) based on high resolution LiDAR DEMs and orthophotos dating from 2004 to
31 2012 (GI 3). To expand the time series of digital glacier inventories in the past, the glacier
32 inventory of the Little Ice Age maximum state (LIA) has been digitalized based on the
33 LiDAR DEM and orthophotos. The resulting glacier area for GI 3 of $415.11 \pm 11.18 \text{ km}^2$ is
34 44% of the LIA area. The annual relative area losses are 0.3 %/year for the ~119 year period
35 GI LIA to GI 1 with one period with major glacier advances in the 1920s. From GI 1 to GI 2
36 (29 years, one advance period in the 1980s) glacier area decreased by 0.6 %/year and from
37 GI2 to GI 3 (10 years, no advance period) by 1.2 %/year . Regional variability of the annual
38 relative area loss is highest in the latest period, ranging from 0.3 to 6.19 %/year. The specific
39 glacier sizes decreased from LIA to the latest period, so that 47% of the glaciers are smaller
40 than 0.1 km^2 in GI 3.

41

42

43 **1 Introduction**

44

45 The history of growth and decay of mountain glaciers affects society in the form of global
46 changes in sea level and in the regional hydrological system as well as through glacier-related
47 natural disasters. Apart from these direct impacts, the study of past glacier changes reveals
48 information on palaeoglaciology and, together with other proxy data, palaeoclimatology and
49 thus helps to compare current with previous climatic changes and their respective effects.

50 Estimating the current and future contribution of glacier mass budgets to sea level rise needs
51 accurate information on the area, hypsography and ice thickness distribution of the world's
52 glacier cover. In recent years the information available on global glacier cover has increased
53 rapidly, with global glacier inventories compiled for the IPCC Report 2013 (Vaughan et al.,
54 2013) complementing the world glacier inventories (WGMS, 2012) and the GLIMS initiative
55 (Kargel et al., 2013). These global inventories serve as a basis for modelling current and
56 future global changes in ice mass (e.g. Gardner et al., 2013; Marzeion et al., 2012; Radić and
57 Hock, 2011). Based on the glacier inventories, ice volume has been modelled with different
58 methods as a basis for future sea level scenarios (Huss and Farinotti, 2012; Linsbauer et al.,
59 2012; Radić et al., 2014). On a regional scale, these glacier inventory data are used for
60 calculating future scenarios of current local and regional hydrology and mass balance (Huss,
61 2012). All this research is based on the most accurate mapping of glacier area and elevation at
62 a particular point in time.

63 For large-scale derivation of glacier surfaces, satellite remote sensing methods are most
64 frequently applied (Paul et al., 2010, 2011b, 2013). For direct monitoring of glacier recession
65 over time, and the linkage of the loss of volume and area to local climatic and ice dynamical
66 changes, time series of glacier inventories are needed. Time series of remote sensing data
67 naturally are limited by the availability of first satellite data (e.g. Rott, 1977), so that time
68 series of glacier inventories have been limited to a length of several decades (Bolch et al.,
69 2010). Longer time series (Nuth et al., 2013; Paul et al., 2011a; Andreassen et al., 2008) can
70 only be compiled from additional data with varying error characteristics (e.g. Haggren et al.,
71 2007) and temporally and regionally varying availability.

72 Although the ice cover of the Alps is not a high portion of the world's ice reservoirs, scientific
73 research on Alpine glaciers has a long history which is important in the context of climate

74 change. Apart from the Randolph glacier inventory data (Ahrendt et al., 2012) and a pan-
75 Alpine satellite-derived glacier inventory (Paul et al., 2011b), several national or regional
76 glacier inventories are available. For Italy, only regional data are available, for example for
77 South Tyrol (Knoll and Kerschner, 2010) and the Aosta region (Diolaiuti et al., 2012). For the
78 five German glaciers, time series of glacier areas have been compiled by Hagg et al. (2012).
79 For the French Alps, glacier inventories have been compiled for 4 dates between 1967/71 and
80 2006/09 by Gardent et al (2014). For Switzerland, several glacier inventories have been
81 compiled from different sources. For the year 2000, a glacier inventory has been compiled
82 from remote sensing data (Kääb et al., 2002; Paul et al., 2004), for 1970 from aerial
83 photography (Müller et al., 1976) and for 1850 the glacier inventory was reconstructed by
84 Maisch et al. (1999). Elevation changes have been calculated between 1985 and 1999 for
85 about 1050 glaciers (Paul and Haeberli, 2008) and recently by Fischer et al. (2014).

86 For the Austrian Alps, glacier inventories so far have been compiled for 1969 (Patzelt, 1980;
87 GI 1) and 1998 (Lambrecht and Kuhn, 2007; GI 2) on the basis of orthophoto maps. Groß
88 (1987) estimated glacier area changes between 1850, 1920 and 1969, mapping the extent of
89 the Little Ice Age (LIA) and 1920 moraines from the orthophotos of the glacier inventory of
90 1969. As the Austrian federal authorities made LiDAR data available for the major part of
91 Austria after years of very negative mass balances after 2000, these data have been used for
92 the compilation of a new glacier inventory based on LiDAR DEMs (Abermann et al., 2010).
93 As the high resolution data allow detailed mapping of LIA moraines, the unpublished maps of
94 Groß (1987) have been used as the basis for an accurate mapping of the area and elevation of
95 the LIA moraines, based on the LiDAR DEMs and the ice divides/glacier names used in the
96 inventories GI 1 and GI 2.

97 The pilot study of Abermann et al. (2009) in the Ötztal Alps identified a pronounced decrease
98 of glacier area, but differing for different size classes. The aim of this study was to update the
99 existing Austrian glacier inventories 1969 (GI 1) and 1998 (GI2) to a GI 3 and complement
100 this as consistently as possible with a LIA inventory based on new geodata (Figure 1) and the
101 mappings of Groß (1987). The overarching research question is the variability of Austrian
102 glacier area changes and change rates by time, region, size class and elevation.

103

104

105 2 Data

106

107

108 2.1 Austrian Glacier inventories

109

110

111 Patzelt (1980) and Groß (1987) derived the first Austrian glacier inventory GI 1 based on
112 orthophotos from 1969 (shape files: Patzelt, 2013). Groß (1987) compiled glacier inventories
113 for the LIA maximum and 1920 from the GI 1 geodata and field surveys mapping the
114 moraines of the respective glacier advances.

115 Lambrecht and Kuhn (2007) used orthophotos between 1996 and 2002 to update the glacier
116 inventory 1969 (GI 1), which they also digitized (Figure 2). In the first, analogue, evaluation
117 of the 1969 orthophotos the glacier area in 1969 was determined as 541.7 km². The glacier
118 areas have been delineated manually by Lambrecht and Kuhn (2007) and Kuhn et al. (2008)
119 as recommended by UNESCO (1970), i.e. snow patches directly attached to the glacier have
120 been mapped as glacier area. The digital reanalysis of the inventory 1969 (GI 1) by
121 Lambrecht and Kuhn (2007) found a total glacier area of 567 km², including also areas above
122 the bergschrund. For the GI 2 (Kuhn et al., 2013), Lambrecht and Kuhn (2007) used the same
123 definition, so that a number of different flight campaigns was necessary to acquire cloud-free
124 orthophotos with a minimum snow cover. Therefore, GI 2 dates from 1996 to 2002, but the
125 main part of the glaciers were covered during the years 1997 (43.5% of the total area) and
126 1998 (38.5% of the total area). Lambrecht and Kuhn (2007) estimated the effect of compiling
127 the glacier inventory from data sources of different years by calculating an area for the year
128 1998. The temporal homogenization of glacier area was done by upscaling or downscaling the
129 recorded inventory area in specific altitude bands with a degree day method to the year 1998.
130 The difference between the recorded area and the area calculated for the year 1998 was only 1.2
131 km². They found a glacier area of 470.9 km² for the summed areas of different dates, and 469.7
132 km² for a temporally homogenized area for the year 1998. All the orthophoto maps and
133 glacier boundaries are published in a booklet (Kuhn et al, 2008), showing also the low amount
134 of snow cover on the orthophotos. The maximum area of the glacier area is estimated to be
135 $\pm 1.5\%$ (Lambrecht and Kuhn, 2007). About 3% of the glacier area of 1969 have not been

136 mapped and several very small glaciers were still missing in GI II. GI I and GI II comprise
137 surface elevation models, with a vertical accuracy of ± 1.9 m (Lambrecht and Kuhn, 2007).

138 **2.2 LiDAR data**

139 Airborne laser scanning is a highly accurate method for the determination of surface elevation
140 in high spatial resolution, allowing the mapping of geomorphologic features, such as moraines
141 (Sailer et al., 2014).

142 The LiDAR DEMs were compiled from a single campaign so that the recorded glacier
143 elevation corresponds to one date only, although the acquisition times of the DEMs differ for
144 the specific mountain ranges. The sensors and requirements on point densities are listed in
145 Table 1. Vertical and horizontal resolution also depends on slope and elevation, nominal mean
146 values for flat areas are better than ± 0.5 m (horizontal) and ± 0.3 m (vertical) accuracy.

147 The point density in one grid cell of 1x1 m ranges from 0.25 to 1 point per square metre. The
148 vertical accuracy depends on slope and surface roughness and ranges from few cm to some
149 dm in very steep terrain (Sailer et al., 2014). LiDAR has a considerable advantage over
150 photogrammetric DEMs where fresh snow or shading reduce vertical accuracy. As the high
151 spatial resolution also reflects surface roughness, smooth ice-covered surfaces can be clearly
152 distinguished from rough periglacial terrain. The flights were carried out during August and
153 September in the years 2006 to 2012, when snow cover was minimal and the glacier margins
154 snow free.

155

156 **2.3 Orthophotos**

157 Orthophotos were used for the delineation of glacier margins where no LiDAR data were
158 available. All orthophotos used are RGB true colour orthophotos with a nominal resolution of
159 20x20 cm. Orthophotos from 2009 were used for Ankogel- Hochalmspitzgruppe,
160 Defreggergruppe, Glocknergruppe, Granatspitzgruppe, the western part of Schobergruppe and
161 the East Tyrolean part of Venedigergruppe. Glacier margins in the eastern part of Zillertaler
162 Alpen and the northern part of Venedigergruppe, located in Salzburg province, were
163 determined using orthophotos from the year 2007. Orthophotos from 2012 were used for
164 Dachsteingruppe.

165

166 **3 Methods**

167

168 **3.1 Applied basic definitions**

169

170 The compilation of the glacier inventory time series aims at monitoring glacier changes with
171 time. Therefore, ice divides and specific definitions regarding what is considered a glacier
172 were kept unchanged, although they could have been changed for compiling single
173 inventories. To make the definitions used in this study clear, the definition of glaciers, as well
174 as glacier area and the separation by ice divides are specified here. Naturally, inventories
175 which serve purposes other than compiling inventory time series will use other definitions,
176 for example mapping changing ice divides instead of constant ones.

177 The ice divides remain unchanged in all glacier inventories and are defined from the glacier
178 surface in 1998. Although ice dynamics are likely to change between the inventories, leaving
179 the position of the divides unchanged has the advantage that no area has shifted from one
180 glacier to another.

181 The parent data set for this study is the GI 1, so that the unique IDs in GI 1 were kept in later
182 inventories. If a glacier had disintegrated in the inventory of 2006, one ID refers to polygons
183 consisting of several parts of a formerly connected glacier area. For the disintegration of
184 glaciers, the parent and child IDs as used in the GLIMS inventories (Raup et al, 2007; Raup et
185 al, 2010) are an excellent solution. Going backwards in time, e.g. to where several parents of
186 the GI 1 are part of a larger LIA glacier, would consequently need the definition of a
187 grandparent or the division of the LIA glacier in different tributaries to allow a glacier-by
188 glacier comparison of area changes.

189 No size limit was applied for the mapping of glaciers in the 2006 inventory, i.e. glaciers
190 whose area has decreased below a certain limit are still included in the updated inventory.
191 This avoids an overestimate of the total loss of ice-covered area as a result of skipping small
192 glaciers included in older inventories. The area of glaciers smaller than 0.01 km², which is
193 often considered as a threshold for including glaciers in inventories, was quantified.

194

195

196 **3.2 Mapping the glacier extent in GI 3 from LiDAR**

197 Abermann et al. (2010) demonstrated in a pilot study for the Ötztal Alps that LiDAR DEMs
198 can be used with high accuracy for mapping glacier area. Figure 3 shows a LiDAR hillshade
199 of glaciers in the Ötztal Alps dating from 2006 with orthofotos in VIS and CIR RGB from
200 2010 for comparison. The update of the glacier shapes from the inventory of 1998 was done
201 combining hill shades with different angles calculated from LiDAR DEMs (Figure 4, location
202 of the subset see Figure 3), analysing the surface elevation changes between the GI 2 and GI 3
203 inventories (Figure 5, location of the subset see Figure 3) and by comparison with orthophoto
204 data, where available. The surface elevation change shows a maximum close to the position of
205 the GI 3 glacier margin and should be zero outside the GI 2 glacier margin (apart from
206 permafrost phenomena or mass movements). The resulting glacier boundaries are shown in
207 Figure 6. Abermann et al. (2010) quantify the accuracy of the areas derived by the LiDAR
208 method to $\pm 1.5\%$ for glaciers larger than 1 km^2 and up to $\pm 5\%$ for smaller ones. The
209 comparison with glacier margins measured by DGPS in the field for 118 points showed that
210 95% of these glacier margins derived from LiDAR were within an 8 m radius of the measured
211 points and 85% within a 4 m radius.

212

213 **3.3 Mapping the glacier extent in GI 3 from orthophotos**

214 Where no LiDAR data was available (cf Figure 1, Table 2), the GI 2 glacier boundaries have
215 been updated with orthophotos. As the nominal resolution of the orthophotos used for the
216 manual delineation of the glacier boundaries is similar to GI 2, the estimated accuracy of the
217 glacier area of $\pm 1.5\%$ is considered to be valid also for GI 3.

218

219 **3.4 Deriving the LIA extent**

220

221 The LIA maximum extents were mapped based on previous mappings by Groß (1987) and
222 Patzelt (1973), which were adapted to fit the moraine positions recorded in modern LiDAR
223 DEMs and orthophotos. Groß and Patzelt mapped the LIA extents of 85% of the Austrian
224 glaciers based on field surveys and the maps and orthophotos of the 1969 glacier inventory.
225 Their analogue glacier margin maps had been stored for several decades and suffered some
226 distortion of the paper, so that the digitalization could not reproduce the position of the

227 moraines according to the LiDAR DEMs. Therefore we decided to remap the LIA glacier
228 areas, basically following the interpretation of Groß and Patzelt, but remaining consistent with
229 the digital data. Figure 7 shows the hillshades of the tongues of Gaißbergferner with
230 pronounced LIA, 1920 and 1980 moraines, which are ice cored on the orographic left side.
231 The basic delineation of Groß (1987) was adapted to fit the LIA moraine in the LiDAR
232 hillshade (Figure 8).

233 Nevertheless, some smaller glaciers, which had wasted down until 1969, might still be
234 missing in the LIA inventory. Groß (1987) accounted for these disappeared glaciers by adding
235 6.5% to the LIA area. We decided to include this consideration in the discussion on
236 uncertainties, although we think that this estimate is fairly accurate.

237

238

239

240 **4 Results**

241 **4.1 Total glacier area**

242 Austrian glaciers cover 941.13 km² (100%) in GI LIA, 564.88 km² (60%) in GI 1, 471.67
243 km² (50%) in GI2 and 415.11 km² (44%) in GI 3 (Table 2). The GI LIA was not corrected for
244 glaciers which completely disappeared before GI 1, so that the area in this study is a bit lower
245 than the 945.50 km² found by Groß (1987). Only four glaciers have wasted down completely
246 between GI 2 and GI 3. Shape files of GI 3 can be downloaded via the Pangaea data base
247 (Fischer, in prep).

248

249 **4.2 Absolute and relative changes of total area**

250 The absolute loss of glacier area, which is interesting from a hydrological perspective, was
251 376 km² between GI LIA and GI 1, 94 km² between GI 1 and GI 2, and 55 km² between GI 2
252 and GI 3 (Table 2). Relative changes of the total area are 40% (GI LIA to GI 1), 17% (GI 1 to
253 GI 2) and 12 % (GI 2 to GI 3). These numbers need a reference to the different period length
254 for a comparison or interpretation, which is usually done by calculating relative changes per
255 year, neglecting glacier advances in the periods. The calculation of annual relative losses
256 between GI LIA and GI 1 is based on the simplification that the LIA maximum occurred in

Kommentar [x1]: Should be ready for
download end of January 2015

257 1850, so that the length of this period is 119 years. Then the relative area change per year is
258 calculated to be 0.3 %/year, neglecting glacier advances around 1920 (Groß, 1987) and the
259 temporal variability of the occurrence of LIA glacier maximum. The area weighted mean of
260 the number of years between GI 1 and GI 2 is 28.7, resulting in an annual relative change of
261 total area of 0.6 %/year. In this period, a high portion of Austrian glaciers advanced (Fischer
262 et al., 2013). The latest period, GI 2 to GI 3, showed a general glacier recession without
263 significant advances, resulting in an annual relative area loss of 1.2%/year for the area
264 weighted period length of 9.9 years. Therefore, overall annual relative area losses in the
265 latest period are twice as large as for GI 1 to GI 2 and four times as large as GI LIA to GI 1.

266

267

268 **4.3 Results for specific mountain ranges**

269 The absolute areas recorded for specific mountain ranges are shown in Figure 9 and Table 2.
270 Highest absolute glacier area decrease between GI 2 and GI 3 was observed in the Ötztaler
271 Alpen (-13.9 km², 24% of total area loss), the Venedigergruppe (-11.7 km², 20.9% of total
272 area loss), Stubaier Alpen (8.2 km², 4.5%) and Glocknergruppe (-8.17 km², 14.6% of total
273 area loss). These mountain ranges contribute 74.2% of the total Austrian glacier area. Their
274 contribution to the area loss is lower than their share of glacier area, and is only 60.4% of the
275 area loss. The contribution of the Ötztaler Alpen, Silvretta, Zillertaler Alpen and Stubaier
276 Alpen to the total Austrian area loss decreased between the LIA and today, the contribution of
277 Glocknergruppe and Venedigergruppe increased by more than 4% of the total area loss for
278 each mountain range. The relative area loss since the LIA maximum differs between the
279 specific groups: Whereas only 11% of the LIA area is left in the Samnaun Gruppe, 51 to 45%
280 of the LIA area is still ice covered in Rätikon, Ötztaler Alpen, Venedigergruppe, Silvretta,
281 Glocknergruppe and Stubaier Alpen (Figure 10).

282

283 While the annual relative area losses in the first period vary between -0.3 and -0.6 %/year, the
284 regional variability of the relative annual area loss in the two latest periods is much higher the
285 later (and shorter) the period (Table 3).

286 The highest annual relative area loss was observed in Karnische Alpen (-4.5%/year),
287 Samnaungruppe (-5.6%/year), and Verwallgruppe (-5.9%/year) for GI 2 to GI 3. These are
288 groups with a high portion of small glaciers.

289

290 **4.4 Altitudinal variability of area changes**

291

292 In GI 2, 88% of the total area was located at elevations between 2600 and 3300 m.a.s.l (Figure
293 11). In GI 3, the proportion of glacier area located at these elevations was still 87%. The
294 largest portion of the area is located at elevations between 2850 and 3300 m.a.s.l (41% in GI 2
295 and 58% in GI 3), 42% of the area was located in regions above 3000 m in GI 2, decreasing to
296 39% in GI 3.

297 The most severe losses took place in altitudinal zones between 2650 and 2800 m.a.s.l., with a
298 maximum in the elevation zone 2700 to 2750 m.a.s.l. Fifty of the area losses took place at
299 altitudes between 2600 and 2900 m.a.s.l. Therefore the main portion of the glacier covered
300 areas are stored in regions above the current strongest area losses.

301

302 **4.5 Area changes for specific glacier sizes**

303 The interpretation of the recorded glacier sizes has to take into account that not all glaciers
304 which are mapped for newer inventories are part of the older inventories, as the total number
305 of glaciers in Table 4 shows. Although some smaller glaciers are missing in GI 1, the number
306 of glaciers smaller than 0.1 km² has been increasing, replacing the area class between 0.1 and
307 0.5 km² as the most frequent one. At the other end of the scale, 11 glaciers were part of the
308 largest size class in GI 1 and only 8 were left in GI 3.

309 For GI 3, the glaciers in the largest size class of 5 – 10 km² cover 41% of the area (Table 4).
310 All other size classes range between 8 and 17% of the total area, but glaciers of the smallest
311 size class cover only 9% of the total glacier area.

312 The percentage of area contributed by very small glaciers (<0.01 km²) is small. In GI 1, 1
313 glacier covers 0.0015% of the total glacier area. In GI 2, 16 very small glaciers cover 0.024%
314 of the total glacier area, and in GI 3 26 very small glaciers contribute 0.033% of the total
315 glacier area.

316

317 **5 Discussion**

318

319 The uncertainties of the derived glacier areas are estimated to be highest for the LIA
320 inventory, and lowest for GI 3. For all glacier inventories, debris cover and perennial snow
321 fields or fresh snow patches connected to the glacier are hard to identify, although including
322 information on high resolution elevation changes and including additional information from
323 different points in time reduces this uncertainty (Abermann et al., 2010). The high-resolution
324 data were only available for GI 3, so that the interpretation of debris and snow can still be
325 regarded as an interpretational range of several percentage points for the area in GI 1 and 2.
326 The nominal accuracy of the method (Abermann et al., 2010) results in an area uncertainty of
327 $\pm 11.2\%$ or $\pm 2.7\%$.

328 For the interpretation of the LIA inventory, temporal and spatial indeterminacy has to be kept
329 in mind. The temporal indeterminacy is caused by the asynchronous occurrence of the LIA
330 maximum extent. In extreme cases the occurrence of the LIA maximum deviated several
331 decades from the year 1850, which is often used as synonymous with the time of the LIA
332 maximum.

333 The spatial indeterminacy varies between accumulation areas and glacier tongues: The
334 moraines which confined the LIA glacier tongues give a good indication for the LIA glacier
335 margins in most cases as they are clearly mapped in the LiDAR DEMs and changing
336 vegetation is visible in the orthophotos. In some cases, lateral moraines standing proud for
337 several decades eroded later, so that the LIA glacier surface will be interpreted as wider, but
338 also lower than it actually was. In some cases, LIA moraines were subject to mass movements
339 caused by fluvial or permafrost activities. In a very few cases, ice cored moraines developed
340 and moved from the original position. Altogether these uncertainties are small compared to
341 the interpretational range at higher elevations, where no significant LIA moraines indicate the
342 ice margins. Moreover, historical documents and maps often show fresh or seasonal snow
343 cover at higher elevations. For example the federal maps of 1816-1821 and 1869-1887 in
344 Figure 12 show surfaces where it is not clear if they are covered by snow, ice or firn.
345 Therefore we cannot even be sure to have included all glaciers which existed during the LIA
346 maximum. Groß (1987) calculated LIA maximum glacier areas of 945.50 km² without, and
347 1011.0 with disappeared glaciers (i.e. 6.5 % disappeared glaciers). According to this estimate,

348 6.5 % of the LIA maximum area is possibly missing from our inventory. Taking this a general
349 mapping error of 3.5% into account we estimate the accuracy of the total ice cover for the
350 LIA as $\pm 10\%$. Figure 12 illustrates that the maps of the third federal survey, together with
351 other historical data, provide some information on the glacier area also in higher elevations. In
352 any investigation of large system changes, as between LIA and today, the definition of the
353 term 'glacier' is difficult, as it is not clear if it makes sense to compare one LIA glacier with
354 the total area of its child glaciers with totally different geomorphology and dynamics, or if it
355 would make more sense to split the LIA glacier into tributaries according to the present
356 situation. Regarding the presented annual rates of area change, it has to be born in mind that
357 all periods apart from GI 2 to GI 3 contain at least one period (around 1920 and in the 1980s)
358 when the majority of glaciers advanced (Groß, 1987; Fischer et al, 2013). Thus a higher
359 temporal resolution of inventories might result in different absolute and relative annual area
360 change rates, as the length change rates, for example during the 1940s, have previously been
361 in the same range as those after 2000.

362 The development of area change rates is similar to the ones found for the Aosta region by
363 Diolaiuti et al., (2012), who arrived at 2.8 km²/year for 1999 to 2005, and 1.1 km²/year for
364 1975 to 1999. The maximum relative area changes in the period of the Austrian GI 2 to GI 3
365 exceed the ones summarized by Gardent et. al. (2014). The periods for which area changes
366 have been calculated for the French Alps by Gardent et al. (2014) are no exact match of the
367 Austrian periods, but the total loss of 25.4% of the glacier area between 1967/71 and 2006/09
368 is similar to the Austrian Alps, despite the higher elevations of the French glaciers. A
369 common finding is the high regional variability of the area changes.

370 Compared to global satellite remote-sensing-based glacier inventories, the glacier inventories
371 presented here show i) high spatial resolution ii) inclusion of additional information iii)
372 minimal snow cover at the time of the flights and iv) consistent nomenclature and ice divides
373 for all four inventories. The high resolution data used in this study is neither available for a
374 global inventory, nor is the high resolution beneficial for global studies, so that global
375 inventories will naturally use satellite remote sensing data. As the Alps often are used as an
376 open space laboratory in glaciology, it nevertheless might make sense to compare results of
377 global inventories with this regional inventory. The Randolph inventory RGI Version 3.2,
378 released 6 September 2013 and downloaded from http://www.glims.org/RGI/rgi_dl.html
379 contains 737 glaciers and a glacier area of 364 km² for the year 2003. These numbers are
380 lower than the ones recorded in the Austrian inventories (GI 2 before 2003 and GI 3 after

381 2003), although cross-border glaciers were not delimited for the comparison. This is clearly a
382 matter of spatial scales, and has no further implication.

383

384 **6 Conclusions**

385

386 This time series of glacier inventories presents a unique document of glacier area change
387 since the Little Ice Age. The regional variability of glacier area loss since the LIA maximum
388 is high, ranging from 89% loss of LIA glacier area for the small glaciers of the Samnaun
389 group to half of the LIA glacier area remaining in a number of other groups. Small groups
390 like Salzburger Kalkalpen and Karnische Alpen show the highest annual losses. The only
391 glacier in Salzburger Kalkalpen region, Übergossene Alm, is currently disintegrating with
392 annual relative area losses of 6.2 %. It seems likely to vanish in the near future. Nevertheless,
393 for some of the largest glacier regions like Stubaier Alpen, Ötztaler Alpen and Silvrettagruppe
394 as well as for the small Rätikon, annual relative changes even in the latest period are smaller
395 than 1%/year. Although generally the relative annual losses increased since the LIA, some
396 groups, for example Silvrettagruppe and Rätikon, exhibit a decrease in the latest period. The
397 reason for that might be found in small scale mass balance variabilities in the shortest period
398 analysed, or topographic or dynamical responses. For a meaningful interpretation of annual
399 relative losses the length of the periods and the occurrence of positive mass balances and
400 advances must be taken into account. We hope that the presented data basis will be used for
401 further studies and investigations of glacier response to climate change.

402

403 **Acknowledgments**

404

405 This study was supported by the federal governments of Vorarlberg, Tyrol, Salzburg, Upper
406 Austria and Carinthia by providing LiDAR data. The Hydrographical Survey of the Federal
407 Government of Salzburg supported the mapping of glaciers in Salzburg. For the province of
408 Tyrol, the mapping of the LIA glaciers was supported by the Interreg 3P CLIM project. We
409 are grateful for the contributions of Ingrid Meran and Markus Goller who supported the
410 project in their bachelor theses. Bernhard Hynek from ZAMG provided the glacier margins of
411 the glaciers in the Goldberggruppe. We thank Gernot Patzelt and Günther Groß for their
412 helpful comments, and the reviewers Mauri Pelto, Siri Jodha Khalsa, and Frank Paul for their
413 suggestions which helped to thoroughly revise the manuscript.

414

415 **References**

- 416 Abermann, J., Fischer, A., Lambrecht, A., and Geist, T.: On the potential of very high-
417 resolution repeat DEMs in glacial and periglacial environments, *The Cryosphere*, 4, 53-
418 65, doi:10.5194/tc-4-53-2010, 2010.
- 419 Abermann, J., Lambrecht, A., Fischer, A., and Kuhn, M.: Quantifying changes and trends in
420 glacier area and volume in the Austrian Ötztal Alps (1969 - 1997 - 2006), *The*
421 *Cryosphere* 3, 205-215. doi:10.5194/tc-3-205-2009, 2009.
- 422 Andreassen, L.M., Paul, F., Kääb, A., and Hausberg, J.E.: Landsat-derived glacier inventory
423 for Jotunheimen, Norway, and deduced glacier changes since the 1930s, *The*
424 *Cryosphere*, 2, 131-145, doi:10.5194/tc-2-131-2008, 2008.
- 425 Bolch, T., Yao, T., Kang, S., Buchroithner, M.F., Scherer, D., Maussion, F., Huintjes, E., and
426 Schneider, C.: A glacier inventory for the western Nyainqentanglha Range and the Nam
427 Co Basin, Tibet, and glacier changes 1976–2009, *The Cryosphere*, 4, 419-433,
428 doi:10.5194/tc-4-419-2010, 2010.
- 429 Diolaiuti, G.A., Bocchiola, D., Vagliasindi, M., D’Agata, C., and Smiraglia, C.: The 1975–
430 2005 glacier changes in Aosta Valley (Italy) and the relations with climate evolution
431 *Progress in Physical Geography*, 36, 764-785, doi:10.1177/0309133312456413, 2012.
- 432 Fischer, A., Patzelt, G., Kinzl, H.: Length changes of Austrian glaciers 1969-2013. Institut für
433 Interdisziplinäre Gebirgsforschung der Österreichischen Akademie der Wissenschaften,
434 Innsbruck, doi:10.1594/PANGAEA.82182, 2013.
- 435 Fischer, A., submitted.: Austrian glacier inventory 2006. doi: submitted.
- 436 Fischer, M., Huss, M., and Hoelzle, M.: Surface elevation and mass changes of all Swiss
437 glaciers 1980–2010, *The Cryosphere Discuss.*, 8, 4581–4617, doi:10.5194/tcd-8-4581-
438 2014, 2014.
- 439 Gardent, M., Rabatel, A., Dedieu, J.-P., and Deline, P.: Multitemporal glacier inventory of the
440 French Alps from the late 1960s to the late 2000s, *Global and Planetary Change*, 120,
441 24-37, ISSN 0921-8181, <http://dx.doi.org/10.1016/j.gloplacha.2014.05.004>, 2014.
- 442 Gardner, A.S., Moholdt, G., Cogley, G., Wouters, B., Arendt, A.A., Wahr, J., Berthier, E.,
443 Hock, R., Pfeffer, W.T., Kaser, G., Ligtenberg, S. R. M., Bolch, T., Sharp, M. J.,
444 Hagen, J.O., van den Broeke, M. R., and Paul, F.: A Reconciled Estimate of Glacier
445 Contributions to Sea Level Rise: 2003 to 2009, *Science* 340, 852-857, doi:
446 10.1126/science.1234532, 2013.
- 447 Groß, G.: Der Flächenverlust der Gletscher in Österreich 1850-1920-1969, *Zeitschrift für*
448 *Gletscherkunde und Glazialgeologie* 23(2), 131 -141, 1987.

449 Hagg, W., Mayer, C., Mayr, E., and Heilig, A.: Climate and glacier fluctuations in the
450 Bavarian Alps during the past 120 years, *Erdkunde*, 66, 121-142, 2012.

451 Haggren, H., Mayer, C., Nuikka, M., Rentsch, H., and Peipe, J.: Processing of old terrestrial
452 photography for verifying the 1907 digital elevation model of Hochjochferner Glacier,
453 *Zeitschrift für Gletscherkunde und Glazialgeologie*, 41, 29-53, 2007.

454 Huss, M., and Farinotti, D.: Distributed ice thickness and volume of all glaciers around the
455 globe, *Journal of Geophysical Research*, 117, F04010, doi: 10.1029/2012JF002523.
456 <http://www.agu.org/pubs/crossref/2012/2012JF002523.shtml>, 2012.

457 Huss, M.: Extrapolating glacier mass balance to the mountain-range scale: The European Alps
458 1900-2100, *The Cryosphere*, 6, 713-727, doi: 10.5194/tc-6-713-2012, [http://www.the-](http://www.the-cryosphere.net/6/713/2012/tc-6-713-2012.html)
459 [cryosphere.net/6/713/2012/tc-6-713-2012.html](http://www.the-cryosphere.net/6/713/2012/tc-6-713-2012.html), 2012.

460 Kääh, A., Paul, F., Maisch, M., Hoelzle, M., and Haerberli, W.: The new remote sensing
461 derived Swiss glacier inventory: II. First results, *Annals of Glaciology*, 34, 362-366,
462 2002.

463 Kargel, J.S., Leonard, G.J., Bishop, M.P., Kaab, A., and Raup, B. (Eds):, *Global Land Ice*
464 *Measurements from Space (Springer-Praxis)*, an edited 33-chapter volume. ISBN: 978-
465 3-540-79817-0, 2013

466 Knoll, C., and Kerschner, H.: A glacier inventory for South Tyrol, Italy, based on airborne
467 laser-scanner data, *Annals of Glaciology*, 50, 53, February 2010, 46-52, 2010.

468 Kuhn, M., Lambrecht, A., Abermann, J., Patzelt, G., and Groß, G.: Die österreichischen
469 Gletscher 1998 und 1969, Flächen und Volumenänderungen. Verlag der
470 Österreichischen Akademie der Wissenschaften, Wien, 2008.

471 Kuhn, M., Lambrecht, A., and Abermann, J.: Austrian glacier inventory 1998. doi:
472 10.1594/PANGAEA.809196, 2013

473 Lambrecht, A., and Kuhn, M.: Glacier changes in the Austrian Alps during the last three
474 decades, derived from the new Austrian glacier inventory, *Annals of Glaciology*, 46,
475 177-184, 2007.

476 Linsbauer, A., Paul, F., and Haerberli W.: Modeling glacier thickness distribution and bed
477 topography over entire mountain ranges with Glab-Top: Application of a fast and robust
478 approach, *J. Geophys. Res.*, 117, F03007, doi: 10.1029/2011JF002313, 2012.

479 Maisch, M., Wipf, A., Denneler, B., Battaglia, J., and Benz, C.: Die Gletscher der Schweizer
480 Alpen. Gletscherhochstand 1850 – Aktuelle Vergletscherung – Gletscherschwund-
481 Szenarien 21. Jahrhundert, Zürich. vdf Hochschulverlag an der ETH Zürich.
482 (Schlussbericht NFP31), 1999.

483 Marzeion, B., Jarosch, A.H., and Hofer, M.: Past and future sea-level change from the surface
484 mass balance of glaciers, *The Cryosphere*, **6**, 1295 - 1322, doi: 10.5194/tc-6-1295-2012,
485 2012.

486 Müller, F., Caflisch, T., and Müller, G.: Firm und Eis der Schweizer Alpen, Gletscherinventar.
487 Zürich, Eidgenössische Technische Hochschule, Geographisches Institut Publ. 57 and
488 57a., 1976.

489 Nuth, C., Kohler, J., König, M., von Deschwanden, A., Hagen, J. O., Käab, A., Moholdt, G.,
490 and Pettersson, R.: Decadal changes from a multi-temporal glacier inventory of
491 Svalbard, *The Cryosphere*, **7**, 1603-1621, doi: 10.5194/tc-7-1603-2013, 2013.

492 Patzelt, G.: Die neuzeitlichen Gletscherschwankungen in der Venedigergruppe (Hohe Tauern,
493 Ostalpen), *Zeitschrift für Gletscherkunde und Glazialgeologie*, **9**, 5-57. 1973.

494 Patzelt, G.: Austrian glacier inventory 1969. doi: 10.1594/PANGAEA.807098, 2013

495 Paul, F., Käab, A., Maisch, M., Kellenberger T., and Haeberli W.: Rapid disintegration of
496 Alpine glaciers observed with satellite data, *Geophys. Res. Lett.*, **31**, L21402, doi:
497 10.1029/2004GL020816, 2004.

498 Paul, F. and Haeberli, W.: Spatial variability of glacier elevation changes in the Swiss Alps
499 obtained from two digital elevation models, *Geophys. Res. Lett.*, **35**, L21502, doi:
500 10.1029/2008GL034718, 2008.

501 Paul, F., Barry, R. G., Cogley, J. G., Frey, H., Haeberli, W., Ohmura, A., Ommanney, C. S.
502 L., Raup, B., Rivera, A., and Zemp, M.: Guidelines for the compilation of glacier
503 inventory data from digital sources, *Annals of Glaciology*, **50** (53), 119-126, 2010.

504 Paul, F., Andreassen, L.M., and Winsvold, S.H.: A new glacier inventory for the
505 Jostedalbreen region, Norway, from Landsat TM scenes of 2006 and changes since
506 1966. *Annals of Glaciology*, **52** (59), 153-162, 2011a.

507 Paul, F., Frey, H., and Le Bris, R.: A new glacier inventory for the European Alps from
508 Landsat TM scenes of 2003: Challenges and results, *Annals of Glaciology*, **52** (59),
509 144-152, 2011b.

510 Paul, F., Barrand, N., Berthier, E., Bolch, T., Casey, K., Frey, H., Joshi, S.P., Konovalov, V.,
511 Le Bris, R., Moelg, N., Nosenko, G., Nuth, C., Pope, A., Racoviteanu, A., Rastner, P.,
512 Raup, B., Scharrer, K., Steffen, S., and Winsvold, S.: On the accuracy of glacier
513 outlines derived from remote sensing data, *Annals of Glaciology*, **53** (63), 171-182,
514 2013.

515 Radić, V., and Hock, R.: Regionally differentiated contribution of mountain glaciers and ice
516 caps to future sea-level rise, *Nat. Geosci.*, **4**, 91-94, doi: 10.1038/ngeo1052, 2011.

517 Radić, V., Bliss, A., Beedlow, A.C., Hock, R., Miles E., and Cogley, J.G.: Regional and
518 global projections of twenty-first century glacier mass changes in response to climate
519 scenarios from global climate models. *Climate Dynamics*, 42, 37-58, 2014.

520 Raup, B.H., Racoviteanu, A., Khalsa, S.J.S. Helm, C. Armstrong, R. and Arnaud, Y.: The
521 GLIMS Geospatial Glacier Database: a new tool for studying glacier change. *Global
522 and Planetary Change*, 56, 101-110, 2007.

523 Raup, B.H., and Khalsa, S.J.S.: GLIMS analysis tutorial, 15 pp. Available at
524 http://www.glims.org/MapsAndDocs/assets/GLIMS_Analysis_Tutorial_a4.pdf, 2010.

525 Rott, H.: Analyse der Schneeflächen auf Gletschern der Tiroler Zentralalpen aus Landsat-
526 Bildern, *Zeitschrift für Gletscherkunde und Glazialgeologie*, 12/1, 1-28, 1977.

527 Sailer, R., Rutzinger, M., Rieg, L., and Wichmann, V.: Digital elevation models derived from
528 airborne laser scanning point clouds: appropriate spatial resolutions for multi-temporal
529 characterization and quantification of geomorphological processes, *Earth Surf. Process.
530 Landforms*, 39, 272-284. doi:10.1002/esp.3490, 2014.

531 UNESCO: Perennial ice and snow masses: a guide for compilation and assemblage of data for
532 a world inventory, UNESCO/IASH Tech. Pap. Hydrol. 1., 1970

533 Vaughan, D.G., Comiso, J.C., Allison, I., Carrasco, J., Kaser, G., Kwok, R., Mote, P., Murray,
534 T., Paul, F., Ren, J., Rignot, E., Solomina, O., Steffen, K., and Zhang, T.: Observations:
535 Cryosphere. In: *Climate Change 2013: The Physical Science Basis. Contribution of
536 Working Group I to the Fifth Assessment Report of the Intergovernmental Panel on
537 Climate Change*, [Stocker, T.F., Qin, D., Plattner, G.-K., Tignor, M., Allen, S.K.,
538 Boschung, J., Nauels, A., Xia, Y., Bex V., and Midgley, P.M. (eds.)]. Cambridge
539 University Press, Cambridge, United Kingdom and New York, NY, USA, 2013.

540 WGMS, and National Snow and Ice Data Center (comps.). *World Glacier Inventory*, Boulder,
541 Colorado USA: National Snow and Ice Data Center.
542 <http://dx.doi.org/10.7265/N5/NSIDC-WGI-2012-02>, 1999, updated 2012.

543

544 Table 1: Sensor and point densities.

	sensor	point density/m ²
Tirol	ALTM 3100 and Gemini	0.25
Salzburg	Leica ALS-50, Optech ALTM-3100	1.00
Vorarlberg	ALTM 2050	2.50
Kärnten-Karnische Alpen	Riegl LMS Q680i and Riegl LMS Doublescansystem	1.00
Kärnten-other	Leica ALS-50/83 and Optech Gemini	1.00

545

546

547

548

549

550

551

552

553

554 Table 2: Acquisition times of the glacier inventories with glacier areas for specific mountain
 555 ranges shown in Figure 1; L means LiDAR ALS data and O means orthophoto.

group	GI II year	GI III year	data source	LIA	GI-I	GI-II	GI-III
				km ²	km ²	km ²	km ²
Allgäuer Alpen	1998	2006	L	0.29	0.20	0.09	0.07
Ankogel- Hochalmspitzgruppe	1998	2009	O	39.94	19.17	16.03	12.05
Dachsteingruppe	2002	2012	O	11.95	6.28	5.69	5.08
Defregger Gruppe	1998	2009	O	2.01	0.70	0.43	0.30
Glocknergruppe	1998	2009	O	103.5 8	68.93	59.84	51.67
Granatspitzgruppe	1998	2009	O	20.08	9.76	7.52	5.48
Karnische Alpen	1998	2009	L	0.29	0.20	0.18	0.09
Lechtaler Alpen	1996	2004/0 6	L	2.09	0.70	0.69	0.55
	1996	2006	L				0.36
	1996	2004	L				0.19
Ötztaler Alpen	1997	2006	L	280.3 5	178.3 2	151.16	137.58
Rätikon	1996	2004	L	3.12	2.19	1.65	1.61
Rieserfernergruppe	1998	2009	L	8.07	4.60	3.13	2.75
Salzburger Kalkalpen	2002	2007	L	5.68	2.47	1.68	1.16
Samnaungruppe	2002	2006	L	0.59	0.20	0.08	0.07
Schoberggruppe	1998	2007/0 9	L/O	9.88	5.60	3.49	2.57
	1998	2007	L				0.96
	1998	2009	O				1.61
Silvretta- gruppe	1996	2004/0 6	L	41.27	23.96	18.97	18.48

		2006	L				9.86
		2004	L				8.62
Sonnblickgruppe	1998	2009	L	24.81	12.76	9.74	7.91
				110.1			
Stubaiier Alpen	1997	2006	L	0	63.05	53.99	49.42
		2007/0		145.2			
Venedigergruppe	1997	9	L/O	0	93.44	81.01	69.31
	1997	2007	O				29.85
	1997	2009	L				39.47
		2004/0					
Verwallgruppe	2002	6	L	13.41	6.70	4.65	4.08
	2002	2006	L				3.66
	2002	2004	L				0.41
		2007/1		118.4			
Zillertaler Alpen	1999	1	L/O	2	65.64	50.64	45.24
	1999	2007	O				4.73
	1999	2011	L				40.51
<hr/>					564.8	470.6	415.4
total area				941.13	8	7	7
% of LIA area			100.00	60.02	50.01	44.15	

556

557

558

559

560 Table 3: Relative and relative annual area changes.

561

group	GI 1-	GI 2 - GI	LIA-GI	GI 2-	GI3-	LIA-GI	GI 1-	GI2-
	GI 2	3	1	GI1	GI2	1	GI2	GI3
	years	years	%	%	%	%/year	%/year	%/year
Allgäuer Alpen	29	8	-31	-55	-22	-0.3	-1.9	-2.8
Ankogel-								
Hochalmspitzgruppe	29	11	-52	-16	-25	-0.4	-0.6	-2.3
Dachsteingruppe	33	10	-47	-9	-11	-0.4	-0.3	-1.1
Defregger Gruppe	29	11	-65	-39	-30	-0.5	-1.3	-2.7
Glocknergruppe	29	11	-33	-13	-14	-0.3	-0.5	-1.2
Granatspitzgruppe	29	11	-51	-23	-27	-0.4	-0.8	-2.5
Karnische Alpen	29	11	-31	-10	-50	-0.3	-0.3	-4.5
Lechtaler Alpen	27	8,10	-67	-1	-20	-0.6	-0.1	-2.2
Ötztaler Alpen	28	9	-36	-15	-23	-0.3	-0.5	-2.6
Rätikon	27	8	-30	-25	-25	-0.3	-0.9	-3.1
Rieserfernergruppe	29	11	-43	-32	-22	-0.4	-1.1	-2.0
Salzburger Kalkalpen	33	5	-57	-32	-18	-0.5	-1.0	-3.5
Samnaungruppe	33	4	-66	-60	-22	-0.6	-1.8	-5.6
Schobergruppe	29	9,11	-43	-38	-19	-0.4	-1.3	-1.8
Silvrettagruppe	27	8,10	-42	-21	-25	-0.4	-0.8	-2.7
Sonnblickgruppe	29	11	-49	-24	-21	-0.4	-0.8	-1.9
Stubai Alpen	28	9	-43	-14	-23	-0.4	-0.5	-2.6
Venedigergruppe	28	10,12	-36	-13	-22	-0.3	-0.5	-2.0
Verwallgruppe	33	2,4	-50	-31	-22	-0.4	-0.9	-5.9
Zillertaler Alpen	30	8,12	-45	-23	-23	-0.4	-0.8	-2.0

562

563 Table 4: Number and areas of glaciers per size class.

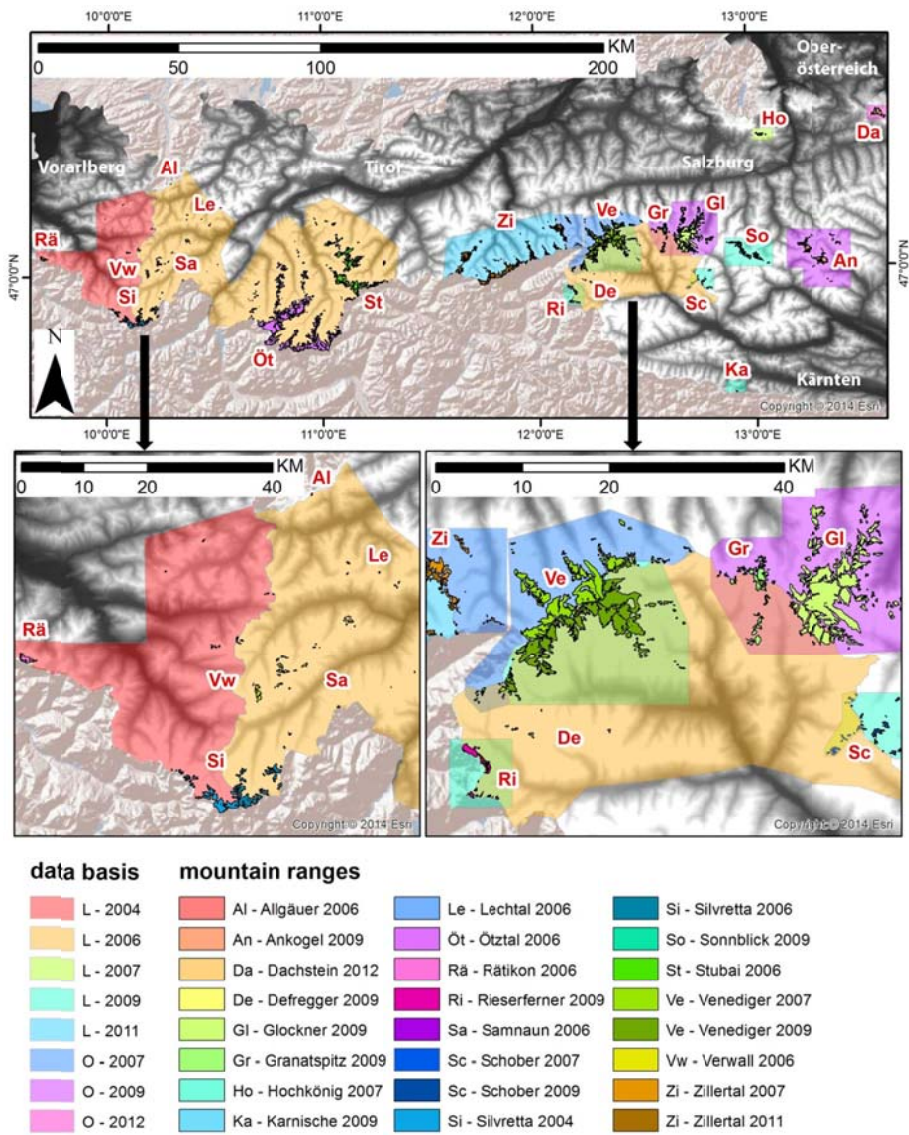
Size classes [km ²]	<0.1	0.1 to 0.5	0.5 to 1	1 to 5	5 to 10	>10	total
	number of glaciers						
in GI 1	177	401	116	99	11	5	809
in GI 2	401	343	92	79	7	3	925
in GI 3	450	307	77	77	8	2	921
% of total area in class							
in GI 1	2	17	14	39	15	13	100
in GI 2	4	17	14	41	14	10	100
in GI 3	5	17	12	41	17	8	100

564

565

567 Figures

568



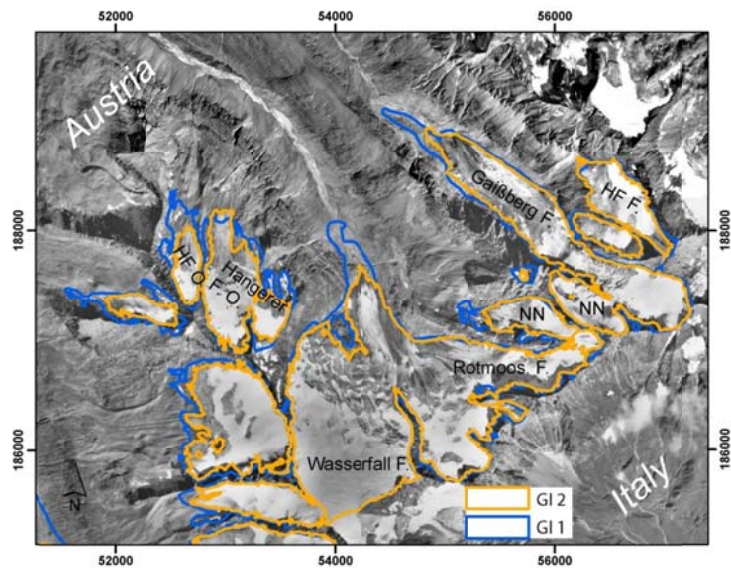
569

569

572 Figure 1: Austrian glaciers displayed on a DEM (Jarvis et al., 2009) color-coded by mountain
573 ranges, with polygons showing data type and date used for deriving GI 3 and GI LIA.

573

574

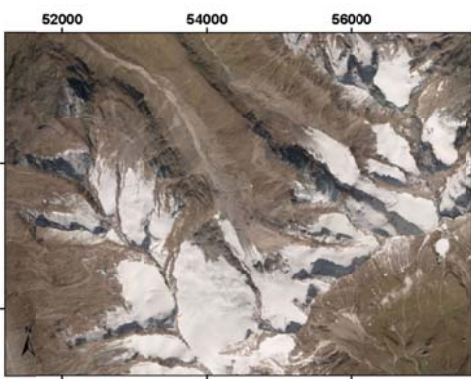
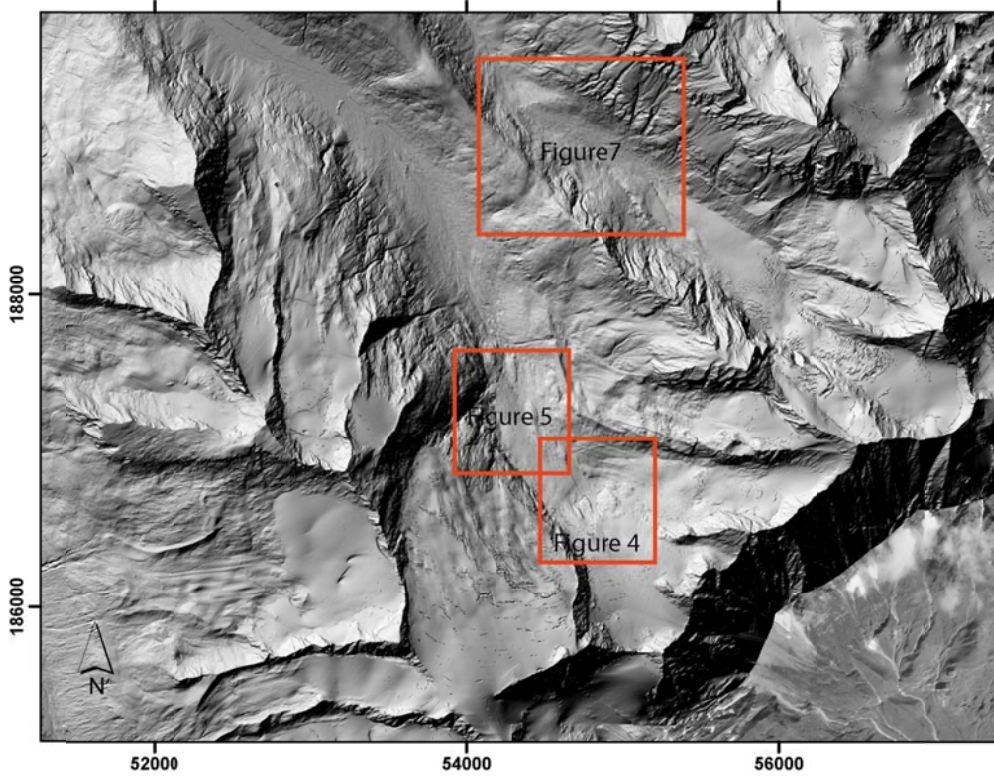


575

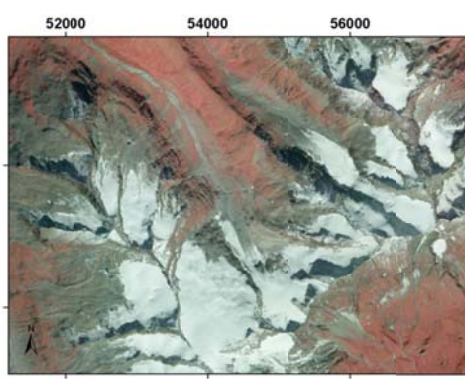
575

579 Figure 2: GI 1 and GI 2 glacier margins superimposed on a GI 2 orthophoto with an oblique
570 photograph of the area in Ötztal Alps. HF O...Hangerer Ferner Ost, HF F...Hochfirst Ferner,
571 NN ...not named.

hillshade GI 3 (2006)



orthofoto RGB VIS 2010



orthofoto RGB CIR 2010

579

580

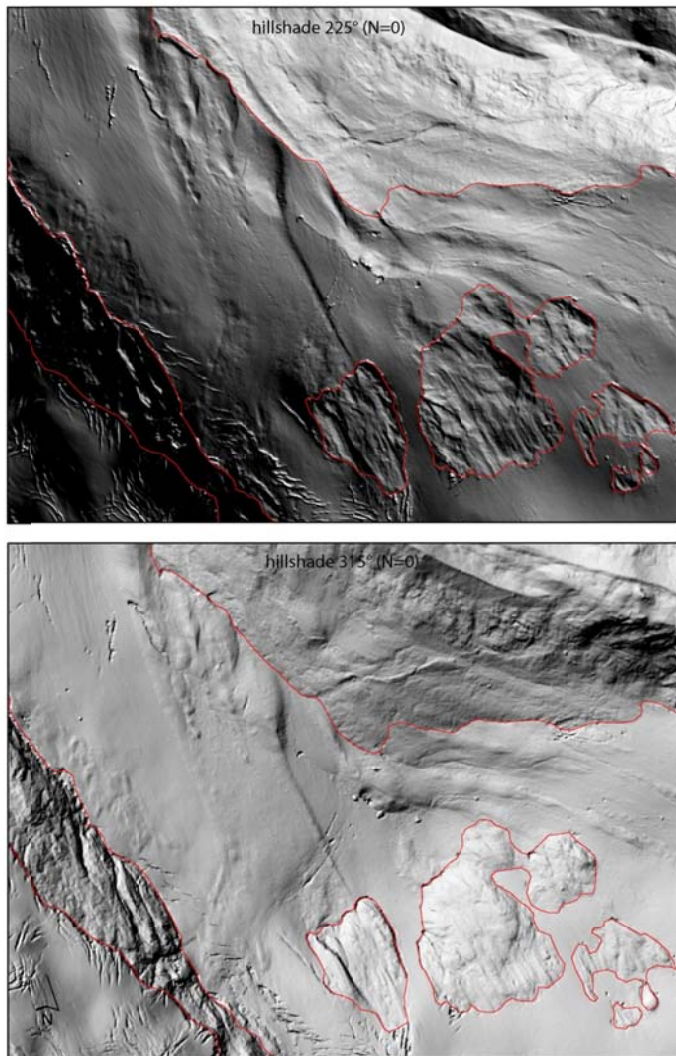
584

585

585

Figure 3: Example of an LiDAR hillshade (2006) of the same area as in Figure 2 with VIS and CIR RGB orthophotos from 2010 for comparison. The inserts show the position of the subsets shown in Figure 4 (lower right rectangle) and Figure 5 (upper left rectangle).

585



587

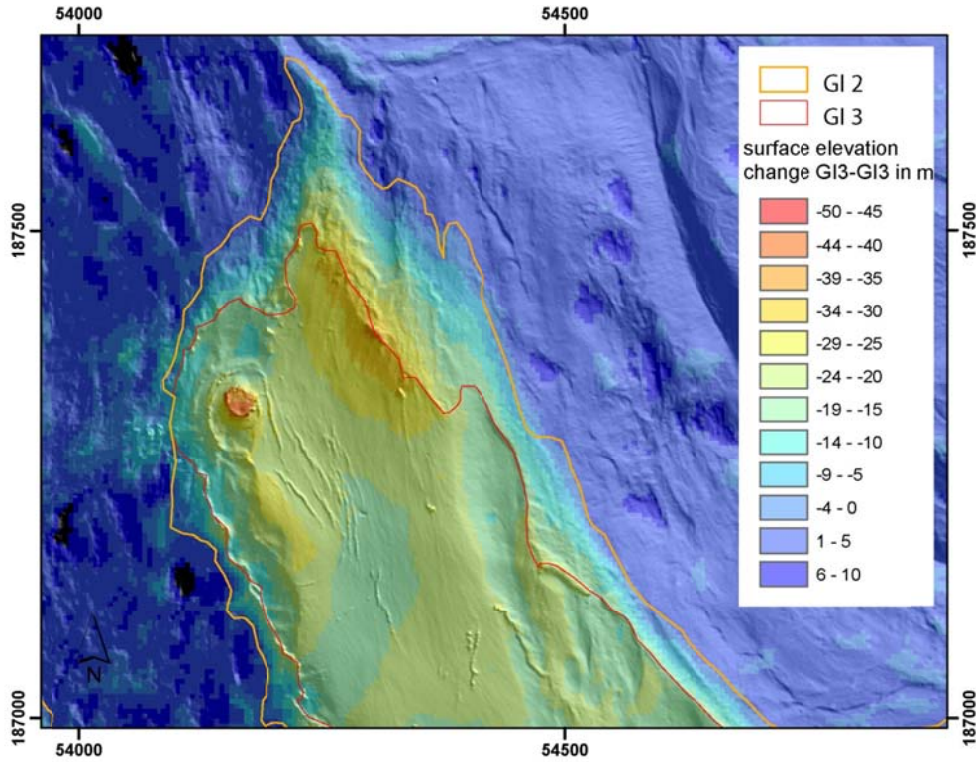
588

589

580

592 Figure 4: Hillshades from different view angles allow to distinguish smooth glacier surfaces
593 from bedrock (position of the subset shown in Figure 3).

593



595

599 Figure 5: The elevation change between GI 2 and GI 3 superimposed on a hillshade shows
590 that the elevation changes can help to delineate the actual (maximum elevation change)
591 previous (outer minimum of elevation change) position of the glacier margin (position of the
592 subset shown in Figure 3).

599

600

602

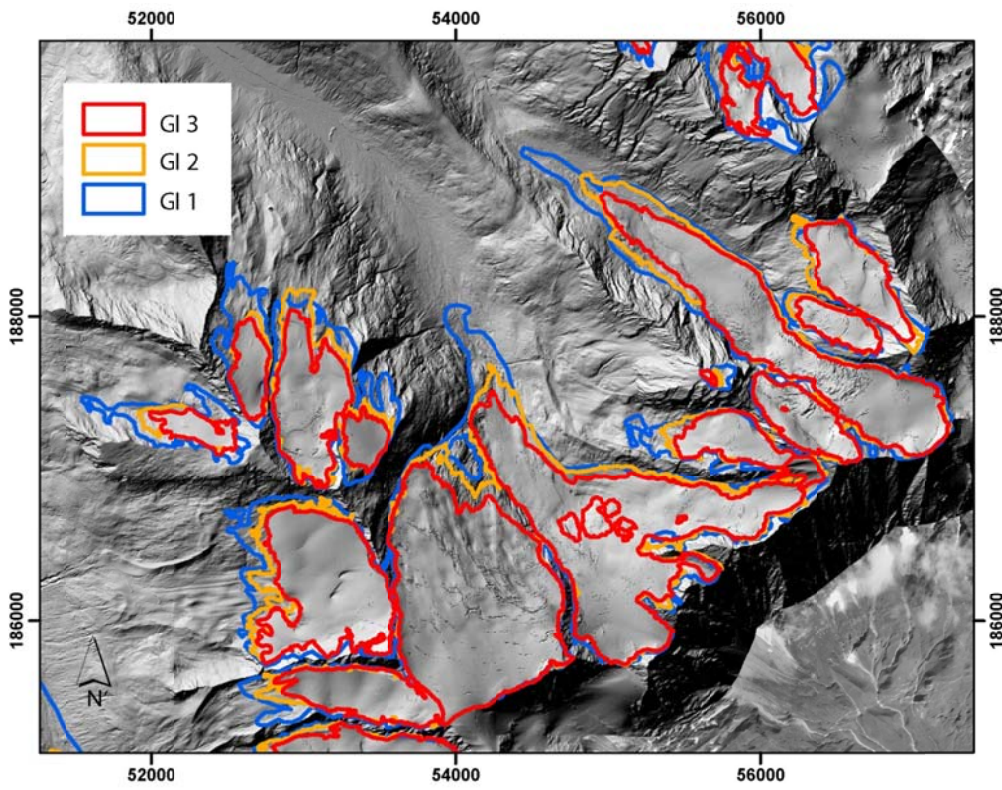
603

604

605

605

607



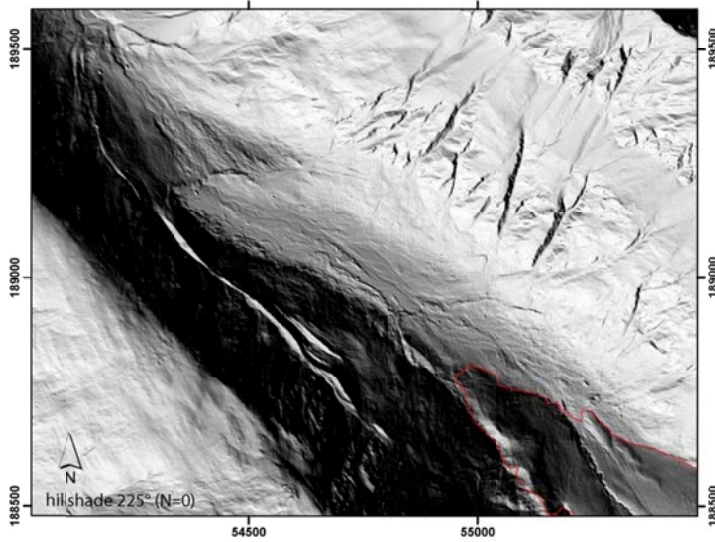
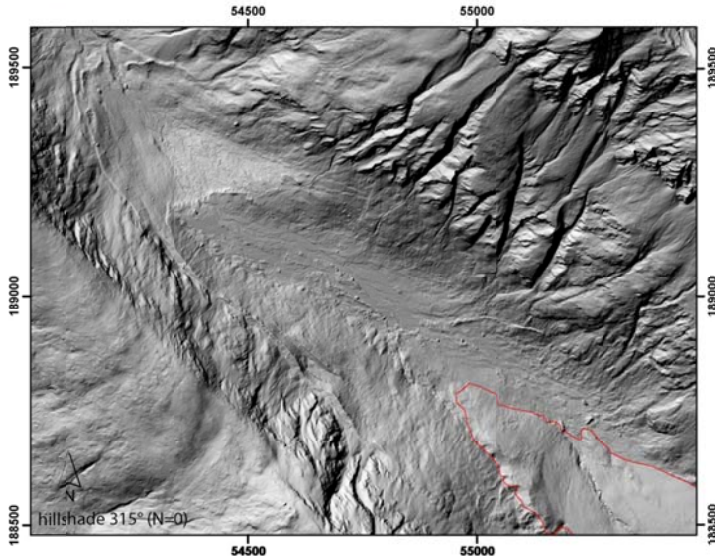
608

600

Figure 6: GI 3 glacier boundaries superimposed on LiDAR hillshade with GI 1 and GI 2 boundaries.

610

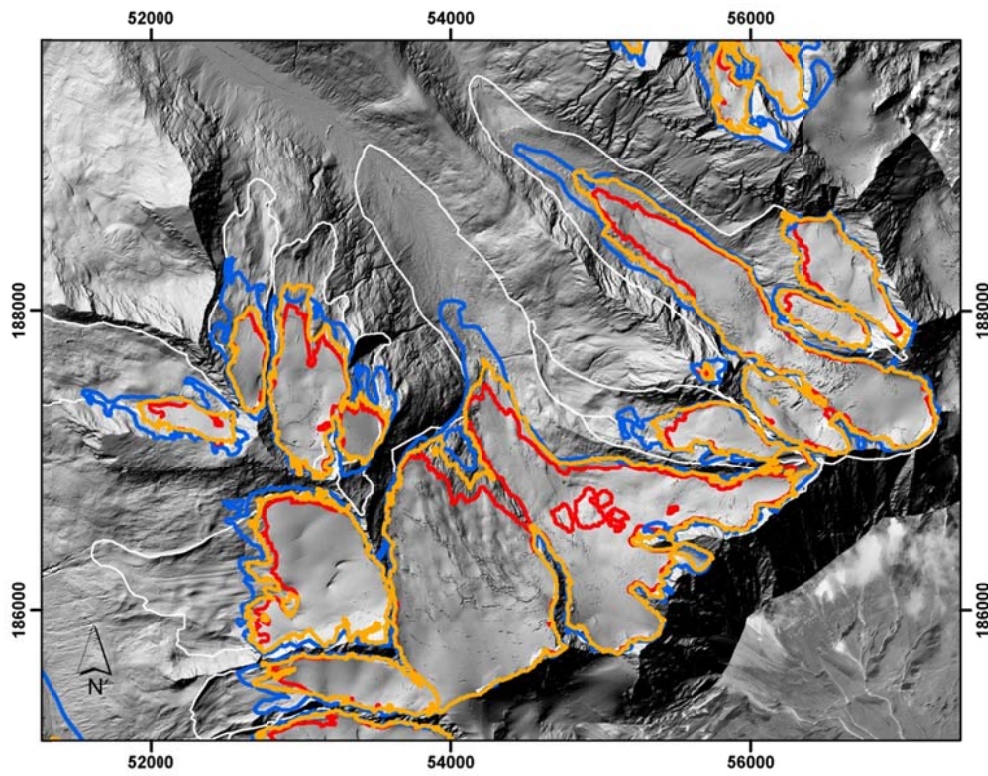
612



613

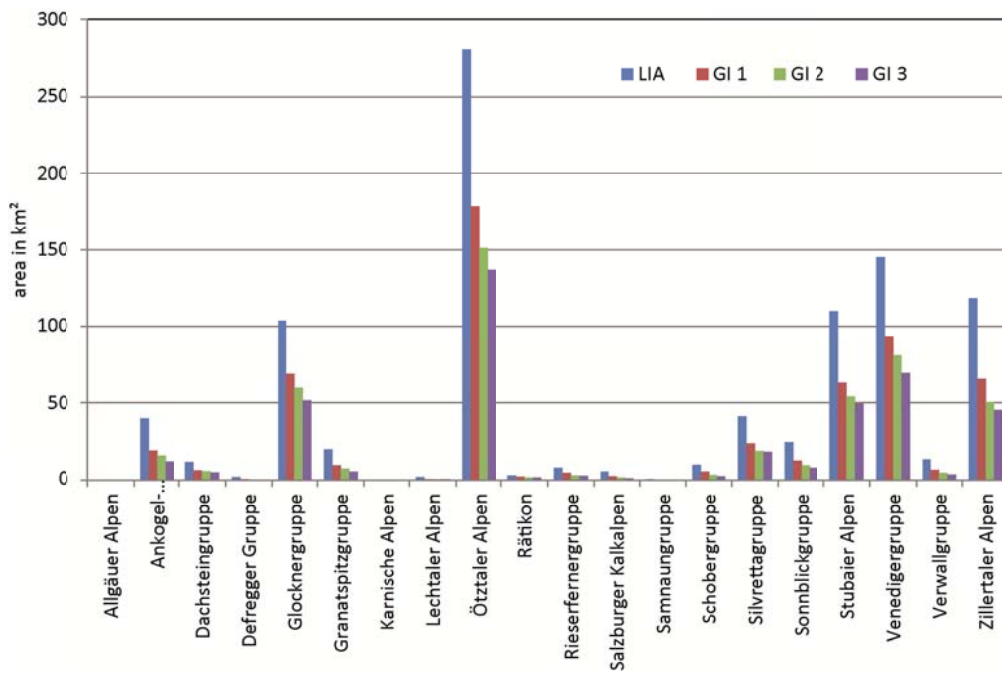
615 Figure 7: Periglacial area of Gaißbergferner with moraines dating from LIA, 1920 and 1980
616 (position of the subset: see Figure 3).

615



617
 619 Figure 8: Resulting LIA glacier areas (white) with several modern glaciers contributing to the
 620 LIA Rotmoos Ferner and LIA Gaißbergferner.

610
 621
 622
 623
 624
 625
 625
 627
 628
 629



620

631

632

633 Figure 9: Glacier areas for specific mountain groups in GI LIA to GI 3.

634

635

635

637

638

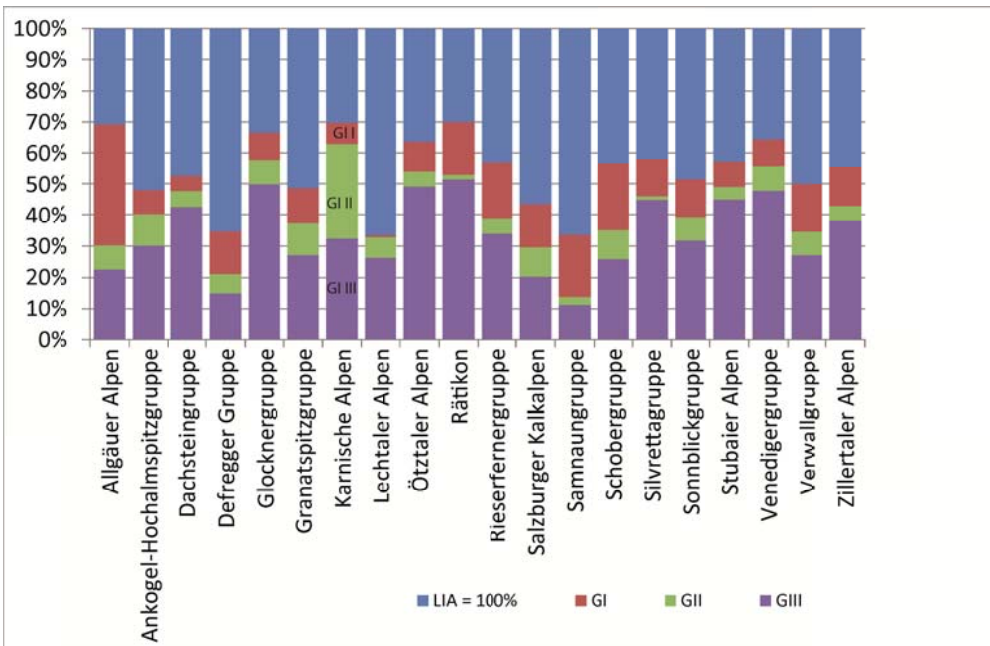
639

639

641

642

643



644

645

645 Figure 10: Area changes of specific mountain ranges in percentage of their LIA area.

647

648

649

640

651

652

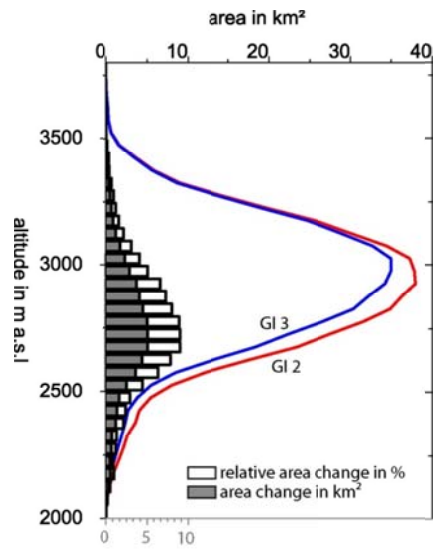
653

654

655

655

657



658

650 Figure 11: Altitudinal distribution of areas in GI 2 and GI 3 with absolute and relative area
 651 changes.

660

662

663

664

665

665

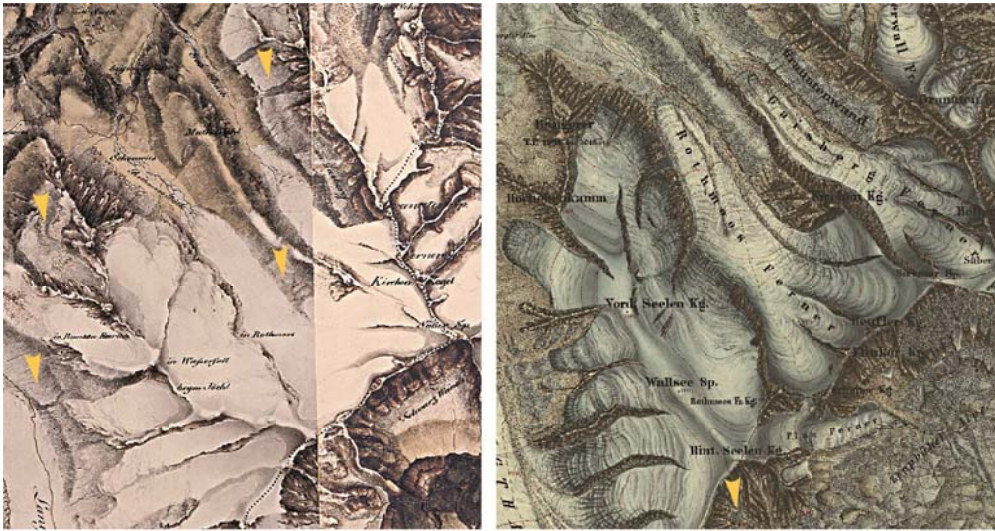
667

668

669

669

670



second federal survey (1816-1821)

third federal survey (1869-1887)

672

675

Figure 12: Federal maps of the second and third federal survey (before and after the LIA maximum) show uncertainties in differentiation of snow, firn and glacier (arrows) but give some general impression on LIA glaciers.

675

677

675

670

673